NONLINEAR CONTINUOUS-DISCRETE OBSERVER APPLICATION TO DISTILLATION COLUMNS

A. C. Téllez-Anguiano[1], C. M. Astorga-Zaragoza[2], E. Alcorta-García[3]
B. Targui[4], E. Quintero-Mármol[2], M. Adam-Medina[2]
and V. H. Olivares-Peregrino[2]

[1]Instituto Tecnológico de Morelia
Av. Tecnológico No. 1500, Col. Lomas de Santiaguito
Morelia, Michoacán 58120, Mexico
adrianat@itmorelia.edu.mx

[2]CENIDET
Interior Internado Palmira s/n, Col. Palmira
Cuernavaca, Morelos 62490, Mexico
{ astorga; eqm; adam; olivares }@cenidet.edu.mx

[3]FIME
Universidad Autónoma de Nuevo León
Avenida Universidad s/n, Cd. Universitaria
San Nicolás de los Garza, N.L., 66450, Mexico
efrain.alcortagr@uanl.edu.mx

[4]GREYC
Université de Caen
UMR 6072 CNRS, ENSICAEN 6 Bd. Marechal Juin
Caen Cedex 14050, France
targub@iutc3.unicaen.fr

ABSTRACT. *In this paper, the composition estimation for the light component in a distillation column is performed experimentally by a continuous-discrete observer. This observer is an extension of a continuous-time constant-gain observer developed for systems having a triangular form. The constant gain allows an easy tuning of the observer and makes it suitable for its implementation in on-line applications. The main advantage of the continuous-discrete approach is to increase the sampling time of the observer. This feature is suitable for systems with slow dynamics. The proposed observer is used to estimate experimentally the molar fractions for a binary mixture (Ethanol-Water) in a distillation column. The estimates performed for the continuous-discrete observer are acceptable using long sampling times appropriated for the distillation process.*
Keywords: Nonlinear systems, Continuous-discrete observer, Distillation column

1. **Introduction.** Observers, also called virtual sensors (when used with hardware A/D systems), are widely used in industrial processes to estimate variables that are not directly measurable due to the nonexistence or high-cost of the suitable sensors. Because these variables are used to perform control and diagnosis in practical applications, the knowledge of the state variables is required.

Observers are also widely used in different control areas, such as observer-based control [1, 2], fault diagnosis [3, 4], fault-tolerant control [5, 6], process monitoring [7] and system identification [8]. Nowadays, several papers dealing with the problem of observability

and the design of nonlinear systems observers involve interesting applications in process engineering, such as bioreactors [9], polymerization reactors [10] and heat exchangers [11].

Several interesting problems arise when the on-line implementation of observers is required. One is how to treat the nonlinear discrete-time observers case. In this sense, a circle-criterion approach to prove stability of discrete-time nonlinear observers is presented in [12]. The authors in [13] present a design procedure of discrete-time observers based on linear matrix inequalities. Discrete-time reduced-order observers are studied in [14, 15], however, it is assumed that the sampling period is constant; in practice, this is not always true.

Continuous-discrete observers for nonlinear systems were introduced for state affine systems in [16, 17]. Some researchers have used this approach as an alternative solution when relatively long-time sampling periods are required. For instance, the authors in [18] propose the use of continuous-discrete interval observers in applications where discrete measurements are rarely available. The adaptive case (state and parameter estimation are performed simultaneously) can be found in [19, 20] with application to polymerization reactors. More recently, in [21] the authors derive stability conditions for this type of observers in MIMO systems based on the Lyapunov stability theory. In the previously cited papers, the gain of the continuous-discrete observer is computed after a coordinates changes of the original nonlinear system.

As far as the authors have knowledge, just a few papers present an experimental validation of continuous-discrete observers. The observer proposed in this paper is an extension of the continuous-time constant-gain observer, presented in [22].

The purpose of this work is to show that the continuous-discrete approach can use longer sampling periods compared with purely discrete-time observers. This fact is evaluated by implementing the observer in a process control interface system. The observer estimates, on-line, the molar fractions of the light component of a binary mixture in a distillation column, the estimation is performed based on discrete measurements. The effectiveness of the method is proved by using long sampling times suitable for the distillation process.

2. **Constant Gain Observer.** In the following sections, superscripts 1 and 2 denote subvectors, i.e., $\boldsymbol{\zeta}(t) = [\boldsymbol{\zeta}^1(t)\ \boldsymbol{\zeta}^2(t)]^T$, whereas superscript T denotes matrix transposition. Subscripts denote the elements of a vector, i.e., $\boldsymbol{\zeta}^j(t) = [\zeta_1^j(t), \zeta_2^j(t), \ldots, \zeta_{n_j}^j(t)]^T$.

Consider the following nonlinear system

$$\begin{cases} \dot{\boldsymbol{\zeta}}^1(t) = \mathbf{f}^1(\boldsymbol{\zeta}(t), \mathbf{u}(t)) + \boldsymbol{\varepsilon}^1(t) \\ \dot{\boldsymbol{\zeta}}^2(t) = \mathbf{f}^2(\boldsymbol{\zeta}(t), \mathbf{u}(t)) + \boldsymbol{\varepsilon}^2(t) \\ \boldsymbol{\varrho}(t) = [\varrho_1(t)\ \varrho_2(t)]^T = \begin{bmatrix} \mathbf{C}_{n_1}\boldsymbol{\zeta}^1(t) & \mathbf{C}_{n_2}\boldsymbol{\zeta}^2(t) \end{bmatrix}^T \end{cases} \tag{1}$$

where the states of the system are grouped into two vectors $\boldsymbol{\zeta}^1(t) \in \mathbb{R}^{n_1}$, $\boldsymbol{\zeta}^2(t) \in \mathbb{R}^{n_2}$; $\mathbf{u}(t) \in \mathbb{R}^m$ is the input vector; $\boldsymbol{\varepsilon}(t)^j \in \mathbb{R}^{n_j}$, $j = 1, 2$ are two unknown and bounded disturbance vectors; $\boldsymbol{\varrho}(t) = [\varrho_1(t)\ \varrho_2(t)]^T \in \mathbb{R}^2$ is the measured output vector; $\mathbf{C}_{n_j} = [1\ 0\ \ldots\ 0] \in \mathbb{R}^{n_j}$, $j = 1, 2$.

$\mathbf{f}^j(t)$, $j = 1, 2$ are globally Lipschitz functions, they are uniformly bounded with respect to the (bounded) state variables $\boldsymbol{\zeta}(t)$ and they have the following triangular structure (for simplicity, time dependency is omitted):

$$\mathbf{f}^1(\boldsymbol{\zeta}, \mathbf{u}) = \begin{bmatrix} f_1^1(\zeta_1^1, \zeta_2^1, \mathbf{u}) \\ f_2^1(\zeta_1^1, \zeta_2^1, \zeta_3^1, \mathbf{u}) \\ \vdots \\ f_{n_1-1}^1(\boldsymbol{\zeta}^1, \mathbf{u}) \\ f_{n_1}^1(\boldsymbol{\zeta}, \mathbf{u}) \end{bmatrix}$$

and

$$\mathbf{f}^2(\boldsymbol{\zeta}, \mathbf{u}) = \begin{bmatrix} f_1^2(\zeta_1^2, \zeta_2^2, \mathbf{u}) \\ f_2^2(\zeta_1^2, \zeta_2^2, \zeta_3^2, \mathbf{u}) \\ \vdots \\ f_{n_2-2}^2(\zeta_1^2, \dots, \zeta_{n_2-1}^2, \mathbf{u}) \\ f_{n_2-1}^2(\boldsymbol{\zeta}^2, \mathbf{u}) \\ f_{n_2}^2(\boldsymbol{\zeta}, \mathbf{u}) \end{bmatrix}$$

2.1. **Continuous-time constant-gain observer.** Consider the following notations

i)

$$\mathbf{A}_{n_j}(t) = \begin{bmatrix} 0 & a_1(t) & 0 & & 0 \\ \vdots & & a_2(t) & & 0 \\ 0 & & & \ddots & a_{n_j-1}(t) \\ 0 & \dots & & 0 & 0 \end{bmatrix} \tag{2}$$

where $a_k(t)$, $k = 1, \dots, n_{j-1}$ are bounded and unknown functions that should satisfy assumption (**H1**):

- **H1:** There exist two finite strictly positive real numbers α, β, such as $\alpha \le a_k(t) \le \beta$.

ii)

$$\mathbf{S}_{n_j} = \begin{bmatrix} s_{11} & s_{12} & 0 & & & 0 \\ s_{12} & s_{22} & \ddots & & & \vdots \\ 0 & \ddots & & \ddots & & 0 \\ \vdots & & & \ddots & & s_{(n_j-1)n_j} \\ 0 & \dots & 0 & & s_{(n_j-1)n_j} & s_{n_j n_j} \end{bmatrix} \tag{3}$$

Lemma 2.1. *As in [22], assume that (**H1**) holds, then for every $\sigma_j > 0$, $j = 1, 2$ there exists a $n_j \times n_j$ Symmetric Positive Definite (S.P.D.) constant matrix $\mathbf{S}_{n_j}$, given in Equation (3) and $\exists \eta_j > 0$ such that*

$$\mathbf{A}_{n_j}^T(t)\mathbf{S}_{n_j} + \mathbf{S}_{n_j}\mathbf{A}_{n_j}(t) - \sigma_j \mathbf{C}_{n_j}^T \mathbf{C}_{n_j} \le -\eta_j \mathbf{I}_{n_j}, \quad \forall t \ge 0; \quad j = 1, 2 \tag{4}$$

where $\mathbf{A}_{n_j}(t)$ is given by Equation (2), $\mathbf{I}_{n_j}$ is the $n_j \times n_j$ identity matrix.

By considering the notations defined above, the following theorem is given:

Theorem 2.1. *Denote by ε the least upper bound of $\|\boldsymbol{\varepsilon}^j(t)\|$, $j = 1, 2$, i.e., $\varepsilon = \sup_{t \ge 0} \|\boldsymbol{\varepsilon}^j(t)\|$ (sup denotes the supremum). Let δ_1, δ_2 two strictly positive constants such that*

$$\frac{2n_1 - 1}{2n_2 - 1}\delta_1 < \delta_2 < \frac{2n_1 + 1}{2n_2 - 1}\delta_1; \tag{5}$$

and $\boldsymbol{\Delta}_{\theta^{\delta_j}} = diag(\theta^{\delta_j}, \theta^{2\delta_j}, \dots, \theta^{n_j \delta_j})$, $j = 1, 2$. Then, there exist two S.P.D. matrices $\mathbf{S}_{n_j}$, $j = 1, 2$ given by Lemma 2.1 such that the system

$$\begin{aligned} \dot{\hat{\boldsymbol{\zeta}}}^1(t) &= \mathbf{f}^1\left(\hat{\boldsymbol{\zeta}}(t), \mathbf{u}(t)\right) - r_1 \boldsymbol{\Delta}_{\theta^{\delta_1}} \mathbf{S}_{n_1}^{-1} \mathbf{C}_{n_1}^T \left(\mathbf{C}_{n_1}\hat{\boldsymbol{\zeta}}^1(t) - \varrho_1(t)\right) \\ \dot{\hat{\boldsymbol{\zeta}}}^2(t) &= \mathbf{f}^2\left(\hat{\boldsymbol{\zeta}}(t), \mathbf{u}(t)\right) - r_2 \boldsymbol{\Delta}_{\theta^{\delta_2}} \mathbf{S}_{n_2}^{-1} \mathbf{C}_{n_2}^T \left(\mathbf{C}_{n_2}\hat{\boldsymbol{\zeta}}^2(t) - \varrho_2(t)\right) \end{aligned} \tag{6}$$

where $r_1 > 0$, $r_2 > 0$; $\theta > 0$; $\exists \lambda_1 > 0$, $\lambda_2 > 0$, $\nu > 0$; is an observer for the system given in Equation (1), such that $\forall \hat{\boldsymbol{\zeta}}(0)$, $\boldsymbol{\zeta}(0)$, $\|\hat{\boldsymbol{\zeta}}(t) - \boldsymbol{\zeta}(t)\| \le \lambda_1 \exp(-\nu t)\|\hat{\boldsymbol{\zeta}}(0) - \boldsymbol{\zeta}(0)\| + \lambda_2 \varepsilon$.

A full demonstration of this theorem is presented in [22]. Note that this observer can be easily implemented because of its constant gain.

2.2. **Discrete observer.** The observer shown in Equation (6) assumes that the measurements are continuously available. However, this is not always the case in industrial applications. If the measurements are digitally available with a sampling time T_s, then a discrete-time version of the observer shown in Equation (6) is obtained by approximating the derivatives. This approximation is performed by using a forward Euler discretization as follows:

$$\hat{\boldsymbol{\zeta}}^1(t_{k+1}) = \hat{\boldsymbol{\zeta}}^1(t_k) + T_s \left[\mathbf{f}^1\left(\hat{\boldsymbol{\zeta}}(t_k), \mathbf{u}(t_k) \right) - r_1 \boldsymbol{\Delta}_{\theta^{\delta_1}} \mathbf{S}_{n_1}^{-1} \mathbf{C}_{n_1}^T \left(\mathbf{C}_{n_1} \hat{\boldsymbol{\zeta}}^1(t_k) - \varrho_1(t_k) \right) \right]$$

$$\hat{\boldsymbol{\zeta}}^2(t_{k+1}) = \hat{\boldsymbol{\zeta}}^2(t_k) + T_s \left[\mathbf{f}^2\left(\hat{\boldsymbol{\zeta}}(t_k), \mathbf{u}(t_k) \right) - r_2 \boldsymbol{\Delta}_{\theta^{\delta_2}} \mathbf{S}_{n_2}^{-1} \mathbf{C}_{n_2}^T \left(\mathbf{C}_{n_2} \hat{\boldsymbol{\zeta}}^2(t_k) - \varrho_2(t_k) \right) \right] \tag{7}$$

where the terms t_k and t_{k+1} are the simplified form of kT_s and $kT_s + T_s$ respectively, and T_s is the sampling time.

The main disadvantage of using discrete-time observers (discretized by the method described above), is that the sampling period T_s of the data acquisition system coincides with the integration step of the observer differential equations shown in Equation (7). If small integration steps are used to solve the differential equations in (7), then small sampling periods T_s will be required. In this case, the observer implementation could not be possible due to technical problems such as: physical limitations of the data acquisition system, time-delays due to the sensors physics and/or the time needed to process data. Many of these problems are solved by using continuous-discrete observers.

2.3. **Continuous-discrete observer.** Consider the continuous-time system with discrete measurements given by:

$$\dot{\mathbf{x}}(t) = \mathbf{f}(\mathbf{x}(t)) + \mathbf{g}(\mathbf{x}(t))\mathbf{u}(t)$$

$$\varrho(t_k) = h(\mathbf{x}(t_k)) \tag{8}$$

where $\mathbf{x}(t) \in \mathbb{R}^n$ is the state vector, $\mathbf{f}(\mathbf{x}(t))$ and $\mathbf{g}(\mathbf{x}(t))$ are two $n \times 1$ smooth vector fields, $\mathbf{u}(t) \in \mathbb{R}^m$ is a measurable input and $\varrho(t_k) \in \mathbb{R}$ is a measurable output correlated to the state by $\varrho(t_k) = h(\mathbf{x}(t_k))$. The term t_k is used to denote discrete-time dependence.

Authors in [16] propose an alternative solution to the state estimation problem which consists in the use of a continuous-discrete observer. This type of observer is suitable when the measurements are available in relatively long sampling periods, see for instance [17, 18]. In [23], it is demonstrated that certain restrictions in the dimension of the sampling period used by a purely discrete observer exist.

The continuous-discrete observer proposed in [16] for the system given in Equation (8) is a recursive algorithm which is given in two steps:

Step 1: A prediction step in the semi-open time interval $t \in [t_k, t_{k+1})$:

$$\dot{\hat{\mathbf{x}}}(t) = \mathbf{f}\left(\hat{\mathbf{x}}(t) \right) + \mathbf{g}\left(\hat{\mathbf{x}}(t) \right) \mathbf{u}(t)$$

$$\dot{\mathbf{S}}(t) = -\theta \mathbf{S}(t) - \mathbf{A}^T \mathbf{S}(t) - \mathbf{S}(t)\mathbf{A} \tag{9}$$

Step 2: A correction step at time $t = t_{k+1}$:

$$\hat{\mathbf{x}}(t_{k+1}) = \hat{\mathbf{x}}(t_{k+1}^-) - \mathbf{K}\left(\hat{\mathbf{x}}\left(t_{k+1}^- \right) \right) \left[h\left(\hat{\mathbf{x}}(t_{k+1}^-) \right) - \varrho(t_{k+1}) \right]$$

$$\mathbf{S}(t_{k+1}) = \mathbf{S}\left(t_{k+1}^- \right) + T_e \mathbf{C}^T \mathbf{C} \tag{10}$$

where T_e is the sampling time and $\mathbf{K}\left(\hat{\mathbf{x}}(t_{k+1}^-) \right)$ is the observer gain which depends on the state $\hat{\mathbf{x}}(t_{k+1}^-)$. $\mathbf{S}(t_{k+1})$ is a symmetric positive definite matrix. The matrix $\mathbf{A}$ is:

$$\mathbf{A} = \begin{bmatrix} 0 & 1 & 0 & 0 \\ \vdots & & 1 & 0 \\ 0 & & 0 & 1 \\ 0 & \dots & 0 & 0 \end{bmatrix}$$

and $\mathbf{C} = [\ 1 \quad 0 \quad \dots \quad 0\ ]$.

The expression t_{k+1}^- represents the limit value of a variable at t_{k+1}, e.g.,

$$\mathbf{S}(t_{k+1}^-) = \lim_{t \to t_{k+1}} \mathbf{S}(t).$$

It can be easily noticed that this observer is composed by *(i)* a mathematical model of the process in the prediction step and *(ii)* a correction term composed by the observer gain and the error of the process output (with respect to the estimated output) in the correction step. By considering this fact, the following proposition is stated.

Proposition 2.1. *Given the continuous-time system with discrete measurements given by:*

$$\begin{cases} \dot{\boldsymbol{\zeta}}^1(t) = \mathbf{f}^1(\boldsymbol{\zeta}(t), \mathbf{u}(t)) + \boldsymbol{\varepsilon}^1(t) \\ \dot{\boldsymbol{\zeta}}^2(t) = \mathbf{f}^2(\boldsymbol{\zeta}(t), \mathbf{u}(t)) + \boldsymbol{\varepsilon}^2(t) \\ \boldsymbol{\varrho}(t_k) = [\varrho_1(t_k)\ \varrho_2(t_k)]^T = \left[\mathbf{C}_{n_1} \boldsymbol{\zeta}^1(t_k)\ \ \mathbf{C}_{n_2} \boldsymbol{\zeta}^2(t_k) \right]^T \end{cases} \tag{11}$$

where the states $\boldsymbol{\zeta}^j(t)$, the input vector $\mathbf{u}(t)$, the disturbance vectors $\boldsymbol{\varepsilon}(t)^j$ and vector fields $\mathbf{f}^j(\cdot)$ $(j = 1, 2)$ are defined similarly to the continuous case, a continuous-discrete observer is given in two steps:

Step 1: A prediction step in the semi-open time interval $t \in [t_k, t_{k+1})$:

$$\begin{aligned} \dot{\hat{\boldsymbol{\zeta}}}^1(t) &= \mathbf{f}^1 \left(\hat{\boldsymbol{\zeta}}(t), \mathbf{u}(t) \right) \\ \dot{\hat{\boldsymbol{\zeta}}}^2(t) &= \mathbf{f}^2 \left(\hat{\boldsymbol{\zeta}}(t), \mathbf{u}(t) \right) \end{aligned} \tag{12}$$

Step 2: A correction step at time $t = t_{k+1}$:

$$\begin{aligned} \hat{\boldsymbol{\zeta}}^1(t_{k+1}) &= \hat{\boldsymbol{\zeta}}^1(t_{k+1}^-) - \mathbf{Q}_{1\theta} \left[\mathbf{C}_{n_1} \hat{\boldsymbol{\zeta}}^1(t_{k+1}^-) - \varrho_1(t_{k+1}) \right] \\ \hat{\boldsymbol{\zeta}}^2(t_{k+1}) &= \hat{\boldsymbol{\zeta}}^2(t_{k+1}^-) - \mathbf{Q}_{2\theta} \left[\mathbf{C}_{n_2} \hat{\boldsymbol{\zeta}}^2(t_{k+1}^-) - \varrho_2(t_{k+1}) \right] \end{aligned} \tag{13}$$

where the observer gains $\mathbf{Q}_{j\theta}$ are given by $\mathbf{Q}_{j\theta} = r_j \boldsymbol{\Delta}_{\theta^{\delta j}} \mathbf{S}_{nj}^{-1} \mathbf{C}_{nj}^T$ for $j = 1, 2$ and $\boldsymbol{\Delta}_{\theta^{\delta j}}$, $\mathbf{S}_{nj}$, $\mathbf{C}_{nj}$ defined in Subsection 2.1.

The tuning parameters of the proposed observer are r_j $(j = 1, 2)$ and θ.

The constant gain is obtained due that the structure of the system in Equation (12) satisfies the conditions given in [22]. Currently, there is not an available research that combines these two results. In this paper, experimental evidence of the operation of the continuous-discrete constant-gain observer is presented. However, formal evidence is required.

3. **Application to a Distillation Column.** In distillation columns, the estimation of the states that are not measurable or that can only be measured through the combination of some state variables is a fundamental problem. One of the most important variables to consider is the composition of the distilled product, which indicates its quality (purity of the product).

Applying control systems in distillation columns requires the continuous information of the molar compositions of the components. The measurement of this variable can be performed through direct analyzers, such as gas chromatograph or refractive index detectors.

Nevertheless, the costs of investment, implementation and maintenance of these techniques, are very high. Thus, some authors (see for instance [24, 25]), propose estimating this variable through secondary measurements (such as temperature and pressure).

Diverse techniques have been developed in order to estimate molar compositions in distillation columns based on the available measurements of temperature, i.e., a neural based soft-sensor is presented in [26], an extended Luenberger observer in [25], an extended Kalman Filter in [27] and a high-gain observer is synthesized in [28].

3.1. **The mathematical model of the distillation column.** A distillation column consists of trays, a condenser and a boiler, (see Figure 1). The condenser is labeled with number 1, the boiler with number n and the intermediate trays are numbered ascending from the condenser to the boiler. The feeding mixture is deposited in the tray number f, named the feeding tray.
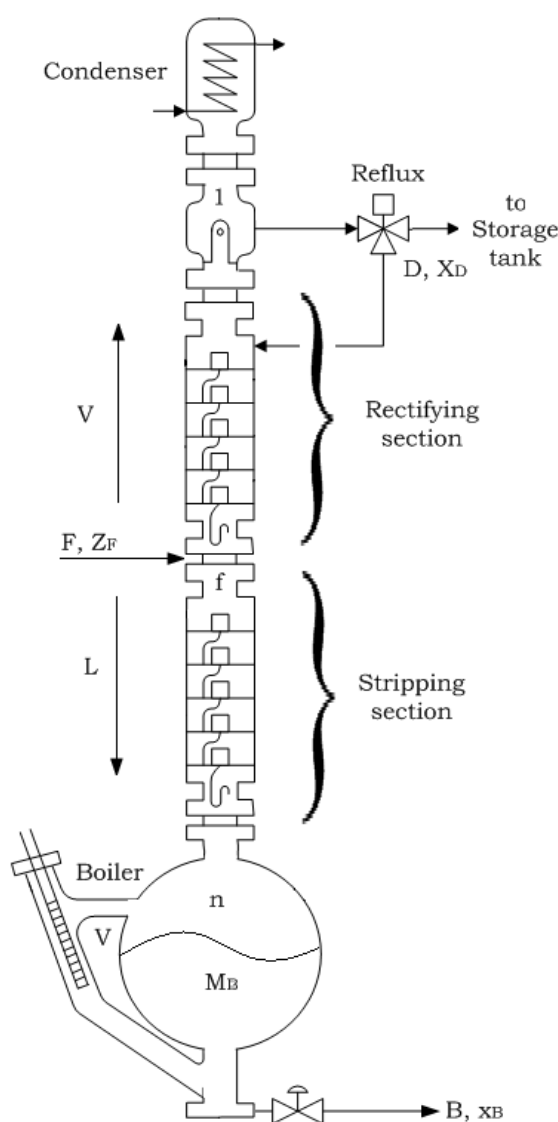

FIGURE 1. Distillation column

The caloric energy is provided by a heating element located in the boiler, which causes the evaporation of the liquid stored into it. The condenser is located in the superior part of the column and its function is to cool and condense the vapor that arrives from the body of the column until it becomes liquid. In this part of the column the reflux is

performed, where everything or a part of the condensed liquid returns to the column to allow the equilibrium phase.

A mathematical model of the system is required to design a state observer; this model provides the structure on which the observer is based.

The following assumptions are considered to model the distillation column:

A1. The mixture is binary (Ethanol-Water).
A2. The components of the mixture are 100 % pure.
A3. The pressure inside the column is constant.
A4. The vapor molar mass is insignificant compared with the liquid molar mass.
A5. The condenser is total.
A6. The molar flow F and the liquid composition x_f of the feeding stream are known.
A7. The process enthalphies are considered constant.
A8. The molar mass retention is considered constant in every tray.

Under the above considerations, the following simplified model is obtained:

$$
\begin{aligned}
M_1 \dot{x}_1 &= V_R(y_2 - x_1) \\
M_p \dot{x}_p &= V_R(y_{p+1} - y_p) + L_R(x_{p-1} - x_p), \quad p = 2, \ldots, f-1 \\
M_f \dot{x}_f &= V_S y_{f+1} - V_R y_f + L_R x_{f-1} - L_S x_f + F x_f \\
M_p \dot{x}_p &= V_S(y_{p+1} - y_p) + L_S(x_{p-1} - x_p), \quad p = f+1, \ldots, n-1 \\
M_n \dot{x}_n &= V_S(x_n - y_n) + L_S(x_{n-1} - x_n)
\end{aligned}
\tag{14}
$$

where x_p and y_p are the liquid and vapor molar fractions (respectively) of the components in every tray. V_p and L_p are the molar flows of the system, which are considered constant and denominated as V_R, V_S, L_R and L_S; subindex R and S correspond to the rectifying and stripping sections of the column, respectively.

3.1.1. *State-space model.* The states of the model are the liquid compositions x_i ($i = 1, \ldots, n$) (it is worth noting that the meaning of n is associated with the context: the dimension of the state or the total number of trays in the column. In the subsequent paragraphs, both interpretations are correct). They can be classified in two vectors:

$$
\mathbf{x}^1(t) = \begin{bmatrix} x_1 \\ x_2 \\ \vdots \\ x_{f-1} \end{bmatrix} \in \mathbb{R}^{n_1} \quad \mathbf{x}^2(t) = \begin{bmatrix} x_n \\ x_{n-1} \\ \vdots \\ x_f \end{bmatrix} \in \mathbb{R}^{n_2}
$$

where clearly $n_1 + n_2 = n$. Physically, the elements of the vectors $\mathbf{x}^1(t)$ and $\mathbf{x}^2(t)$ represent the liquid compositions in the rectifying and the stripping sections respectively.

The two control variables are $\mathbf{u}(t) = [u_1(t) \ u_2(t)]^T = [V \ L]^T$. These input variables can be manipulated by varying the heating power applied on the boiler $Q_b(t)$ and the opening period of the reflux valve $r_v(t)$ respectively.

If the top and the bottom product compositions x_1 and x_n can be measured, then the measured output vector is $\boldsymbol{\varrho}(t) = [\varrho_1(t) \ \varrho_2(t)]^T = [x_1(t) \ x_n(t)]^T$.

The above notations lead to the following compact representation of the dynamical mathematical model of the distillation column, considering discrete-time measurements:

$$
\begin{aligned}
\dot{\mathbf{x}}^1(t) &= \mathbf{f}^1(\mathbf{x}(t), \mathbf{u}(t)) \\
\dot{\mathbf{x}}^2(t) &= \mathbf{f}^2(\mathbf{x}(t), \mathbf{u}(t)) \\
\boldsymbol{\varrho}(t_k) &= [\mathbf{C}_{n_1} \mathbf{x}^1(t_k) \ \mathbf{C}_{n_2} \mathbf{x}^2(t_k)]^T
\end{aligned}
\tag{15}
$$

where $\mathbf{x}(t) = [\mathbf{x}^1(t) \ \mathbf{x}^2(t)]^T \in \mathbb{R}^n$, and

$$\mathbf{f}^1(\mathbf{x}, \mathbf{u}) = \begin{bmatrix} f_1^1(x_1^1, x_2^1, \mathbf{u}) \\ f_2^1(x_1^1, x_2^1, x_3^1, \mathbf{u}) \\ \vdots \\ f_{n_1-1}^1(\mathbf{x}^1, \mathbf{u}) \\ f_{n_1}^1(\mathbf{x}, \mathbf{u}) \end{bmatrix}$$

$$\mathbf{f}^2(\mathbf{x}, \mathbf{u}) = \begin{bmatrix} f_1^2(x_1^2, x_2^2, \mathbf{u}) \\ f_2^2(x_1^2, x_2^2, x_3^2, \mathbf{u}) \\ \vdots \\ f_{n_2-2}^2(x_1^2, \ldots, x_{n_2-1}^2, \mathbf{u}) \\ f_{n_2-1}^2(\mathbf{x}^2, \mathbf{u}) \\ f_{n_2}^2(\mathbf{x}, \mathbf{u}) \end{bmatrix}$$

$$\mathbf{C}_{n_j} = [1 \ 0 \ 0 \ \ldots \ 0] \quad (j = 1, 2)$$

4. **Observer Implementation and Results.** Considering the distillation column model given in Equation (15) the following assumptions are physically verified:

 A9. The flow rates are physically bounded.
A10. The liquid compositions $x_p \in [0, 1]$.

The nonlinear model presented in Equation (15) has the same form than the system given in Equation (11), where the states $\boldsymbol{\zeta}(t)$ are replaced by $\mathbf{x}(t)$ and the disturbances $\boldsymbol{\varepsilon}^j(t) = 0$, $j = 1, 2$ (usually, F and x_f are assumed known, see assumption A6). Then, according to the Proposition 2.1 given in Subsection 2.3, the discrete observer given by Equation (6) and the continuous-discrete observer given by Equations (9) and (10) allow estimating the molar compositions $x_1 \ldots x_n$, based on the measurement of the top and the bottom molar compositions ($x_1(t) = \varrho_1(t)$ and $x_n(t) = \varrho_2(t)$, respectively).

To validate the discrete and continuous-discrete observers performance, several on-line experiments were developed in the distillation pilot plant. A typical operation is presented in this paper. In order to implement (on-line) the proposed observer, a process control interface system was developed by using an adequate instrumentation software.

4.1. **Process control interface brief description.** The process control interface for a distillation process, is an on-line application that has the advantage of supervising the behavior of the process variables and manipulating the actuators of a distillation pilot plant. The graphic interface of the developed station is shown in Figure 2.

By using this interface the user can access different subprograms, through a button menu, in order to execute a desired action over the distillation plant, such as monitoring the temperature, heating the resistors and controlling the reflux valve. This interface has the aim of improving the quality of the distilled product, enhancing the process behavior and increasing the security level of the column.

The user can access the observer program through the menu button that is circled in red in Figure 2.

A special graphic interface was developed to show the estimation results obtained through the observer execution (see Figure 3). This interface presents the on-line estimation of the molar compositions of the system. These estimations are based on the available temperature measurements of the distillation plant.

The graphic interface allows the user to choose the variable to be displayed: estimated temperatures, estimated compositions or measured temperatures. The user can select from one to n trays to be displayed in the window, in order to visualize the estimated and
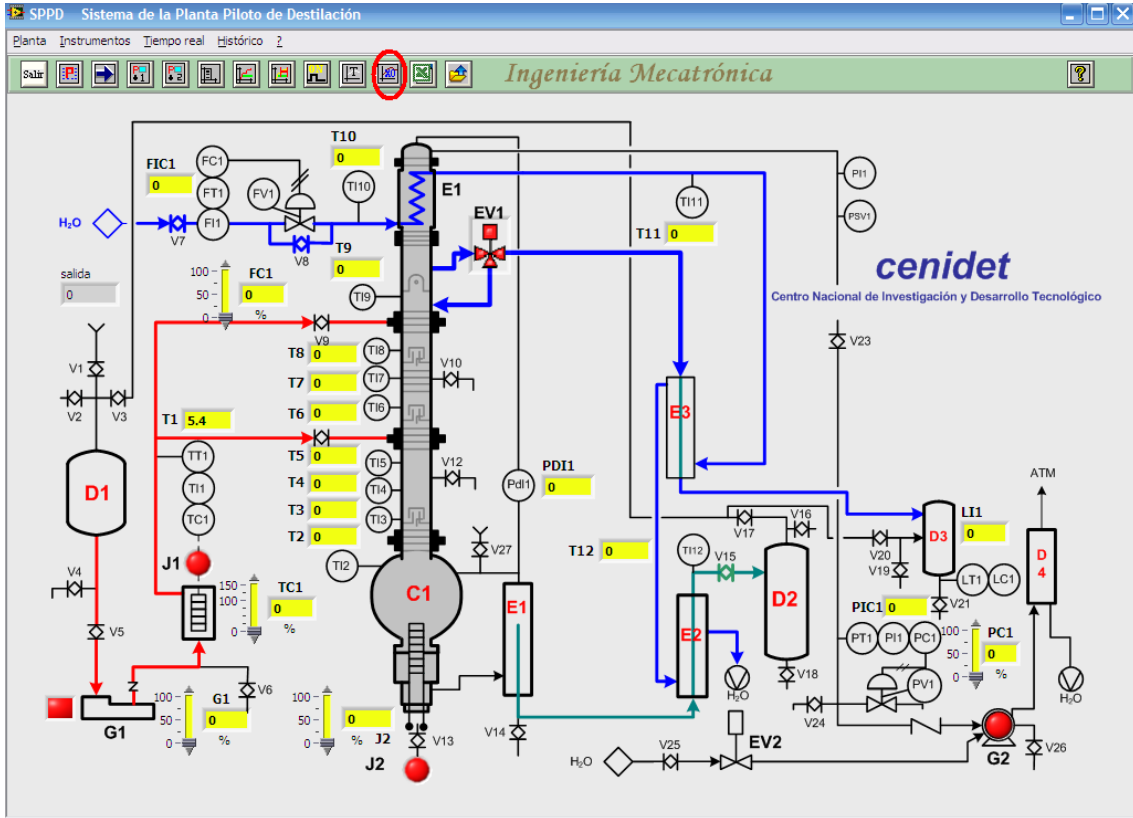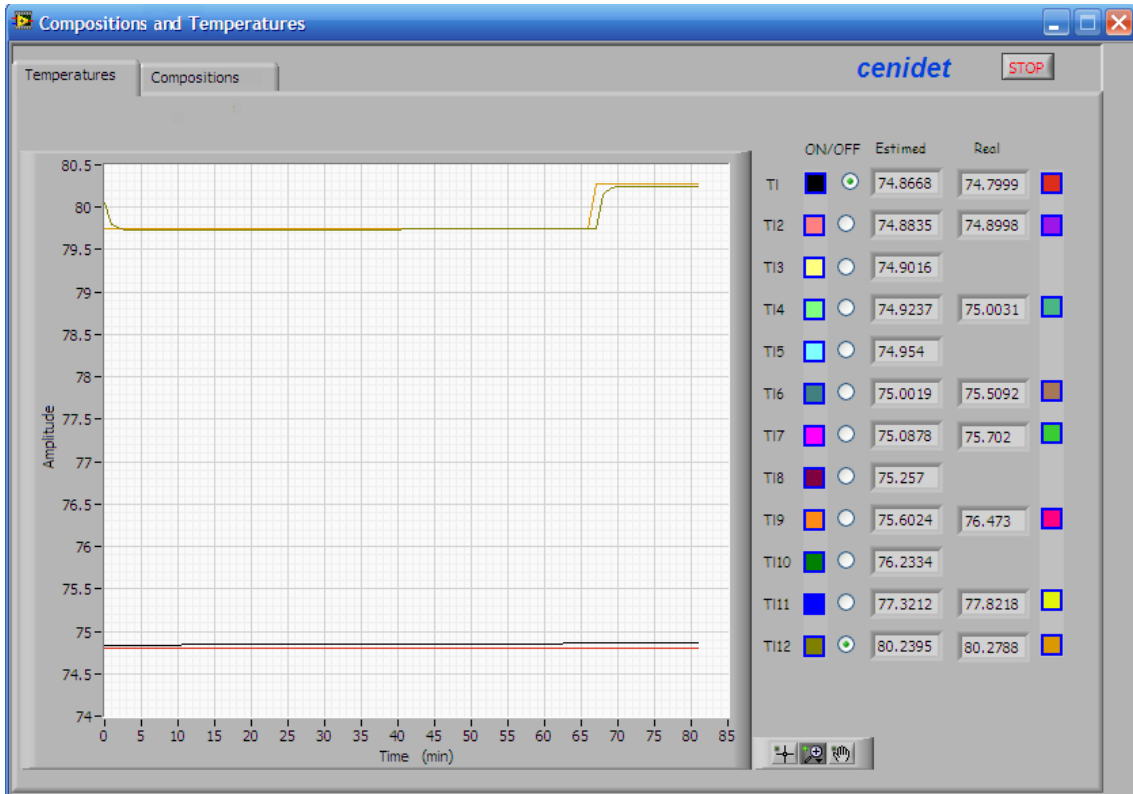
FIGURE 2. Process control interface

FIGURE 3. Observer graphic interface

measured variables comparison. Besides, it presents, on-line, the numerical value of the desired variable. A complete description of this interface can be found in [29].

4.2. **Experimental results.** The distillation column consists of $n = 12$ trays (including the boiler and the condenser); it can be used in batch or continuous operation.

The temperature measurements are available in trays 1, 2, 4, 6, 7, 9, 11 and 12, through 8 Pt-100 RTD sensors. The measurements used in the observer correspond to the boiler (tray 12) and the condenser (tray 1).

The physical variables that can be considered as manipulable inputs in the column are: the heating power of the boiler (0-2500 watts) and the reflux rate. These variables allow controlling the liquid and vapor molar compositions of the light component. The flow, molarity and temperature in the feeding mixture are the perturbations of the process, and they are considered known (in accordance with assumption A6).

The mixture used in this study is Ethanol-Water, characterized as a non-ideal mixture, due that its components form an azeotrope. The thermodynamic properties of the mixture are given in Table 1. The initial operation conditions used for the experiment are presented in Table 2.

TABLE 1. Ethanol and water thermodynamic properties

Parameter	Ethanol	Water	Units
Density (ρ_i)	0.789	1	g/cm^3
Molecular weight (W_i)	46.069	18.015	g
Boiling Temperature (T_{b_i})	78.400	100	$°C$
Specific heat (C_{p_j})	0.112	0.076	kJ/mol $°C$

TABLE 2. Initial operating conditions

Parameter	Value	Units
Ethanol volume in the boiler	3700	ml
Water volume in the boiler	300	ml
Boiler heating power	1250	watts
Cooling liquid flow	250	L/h
Pressure	84.92	kPa

Because the main objective of this work is to estimate the light component composition, the initial composition is settled in 0.7919 in order to determine if the observer is capable of estimate small changes in the trays compositions under high-composition conditions.

The azeotrope characteristics limit the operating range in a simple distillation process (maximum composition = 0.89 – under the experiment pressure conditions).

Table 3 presents the operating conditions used to validate the observer under changing conditions. The events (changes in a process input or perturbation) are presented in chronological order. Recall that the heating power $Q_b(t)$ affects the control variable V, and the reflux rate $r_v(t)$ affects the control variable L. It can be noticed that the heating power Q_b is increased once during the experiment. The reflux variable r_v is manipulated via an on-off valve. When the valve is turned *off*, all the distillate is returned to the column (*Total* reflux), whereas, when the valve is turned *on*, all the distillate is withdrawn from the condenser. The *Pulse* legend in Table 3 means that the reflux valve sequentially turns *on* and *off* every 3s.

TABLE 3. Process inputs and perturbations

Input	Value	Execution time
Q_b	1250 watts	0 min
r_v	Total	0 min
Q_b	1500 watts	53 min
Q_b	1750 watts	72 min
r_v	Pulse ($t_{on} = 3s$, $t_{off} = 3s$)	90 min
r_v	Total	100 min
Q_b	1500 watts	108 min
Q_b	1250 watts	128 min

The continuous-discrete observer given by Equations (12) and (13) was implemented in the process control interface described in Subsection 4.1. The measured process outputs were the temperatures in trays 1 and 12. These temperatures were used to calculate the observer inputs $\varrho_1(t) = x_1(t)$ and $\varrho_2(t) = x_{12}(t)$ by means of the thermodynamic properties of the mixture [30]. The integration of the continuous differential equations was carried out using a Runge-Kutta first order method (Euler) with an integration step of $0.05s$. The design parameters of the observer were $n_1 = 6$, $n_2 = 6$. The values $\delta_1 = 1$, $\delta_2 = 1.29$ were selected to satisfy Equation (5). The tuning parameters were $\theta = 2$, $r_1 = 3$, $r_2 = 3$. These values allow to compute $\mathbf{\Delta}_{\theta^{\delta_j}} = diag(\theta^{\delta_j}, \theta^{2\delta_j}, \ldots, \theta^{n_j \delta_j})$. An adequate S.P.D. matrix $\mathbf{S}_{n_1} = \mathbf{S}_{n_2}$ that satisfies Equation (4) is:

$$S_{n_j} = \begin{bmatrix} 1 & -1 & 0 & 0 & 0 & 0 \\ -1 & 2 & -1.5 & 0 & 0 & 0 \\ 0 & -1.5 & 4 & -2 & 0 & 0 \\ 0 & 0 & -2 & 8 & -3 & 0 \\ 0 & 0 & 0 & -3 & 10.5 & -4 \\ 0 & 0 & 0 & 0 & -4 & 15.5 \end{bmatrix}$$

The initial conditions of the observer were

$$\hat{\mathbf{x}}^1(0) = [\hat{x}_1(0), \ldots, \hat{x}_6(0)]^T = [0.88 \ 0.87 \ 0.865 \ 0.862 \ 0.86 \ 0.85]^T$$

$$\hat{\mathbf{x}}^2(0) = [\hat{x}_{12}(0), \ldots, \hat{x}_7(0)]^T = [0.79 \ 0.795 \ 0.8 \ 0.82 \ 0.84 \ 0.8417]^T$$

The initial conditions do not affect the observer convergence; the observer converges independently of their value. However, these conditions and the discrete sampling time affect the time in which the observer reaches the reference signal; a bigger difference between these values (initial and reference) implies a bigger convergence time.

In order to validate the continuous-discrete observer performance, its response was compared to the discrete observer response under different discrete sampling periods. Figures 4 to 6 show the results obtained in trays 1, 3 and 12 when T_s (discrete observer) and T_e (continuous-discrete observer) are equal to $3s$. The first two figures belong to the rectifying section and the last to the condenser (distilled product) of the column.

These figures show the measured compositions (solid lines) and the compositions estimated by the observer $\hat{x}_i$ (dotted lines). The upper figure corresponds to the discrete observer, the lower belongs to the continuous-discrete observer. The graphics were edited in Matlab®. As expected, the variations on the molar concentrations reflect the variations on the operating conditions. The variations on the measured data is due to the opening and closure of the reflux valve.

These results allow appreciating that the observer estimates are quite acceptable, even near the azeotrope condition and under small value measurement changes, (error less than
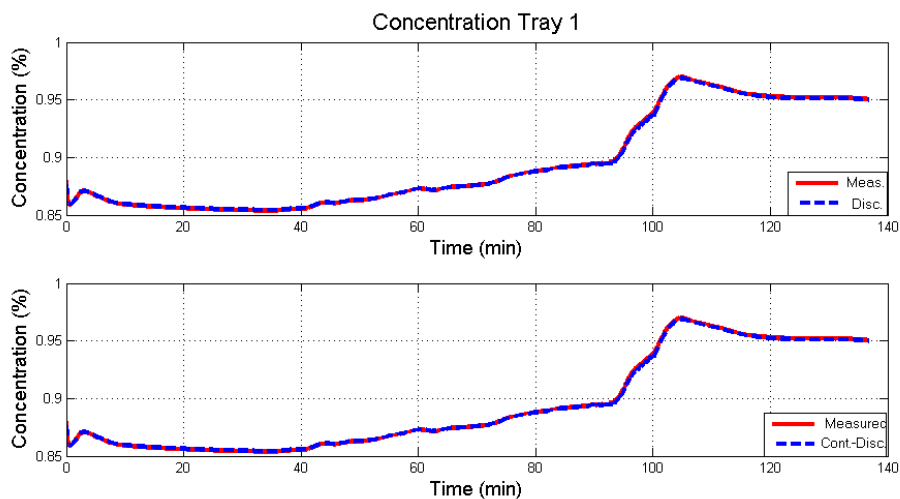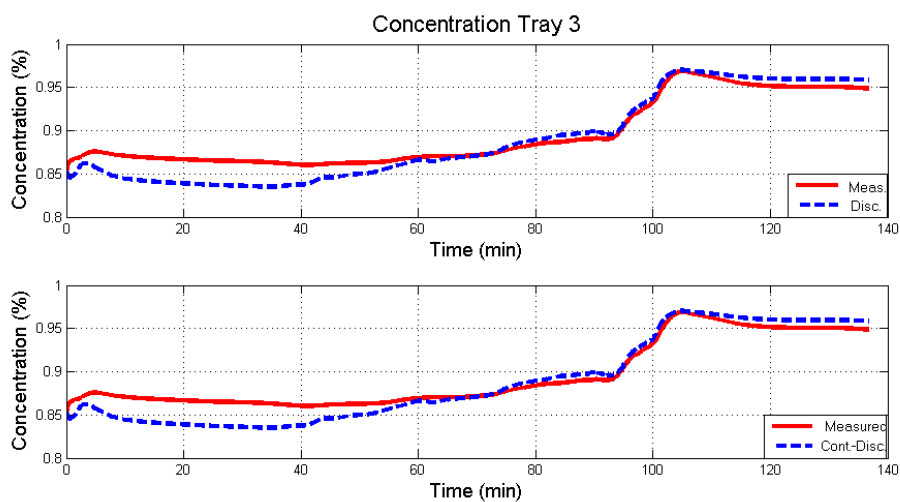
FIGURE 4. Liquid composition in tray 1 ($T_s = T_e = 3s$)

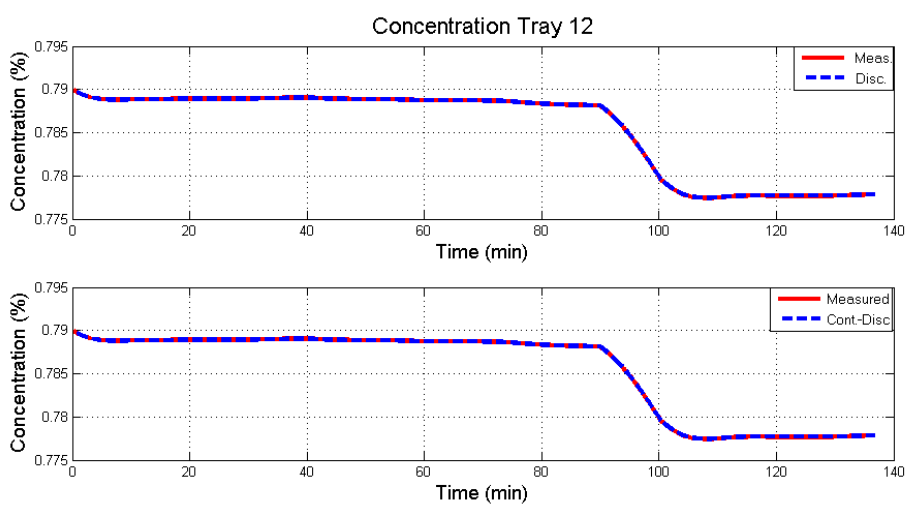

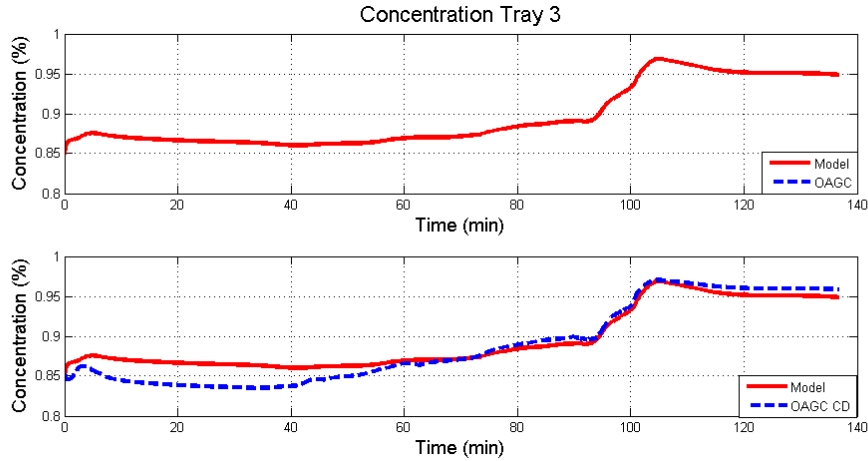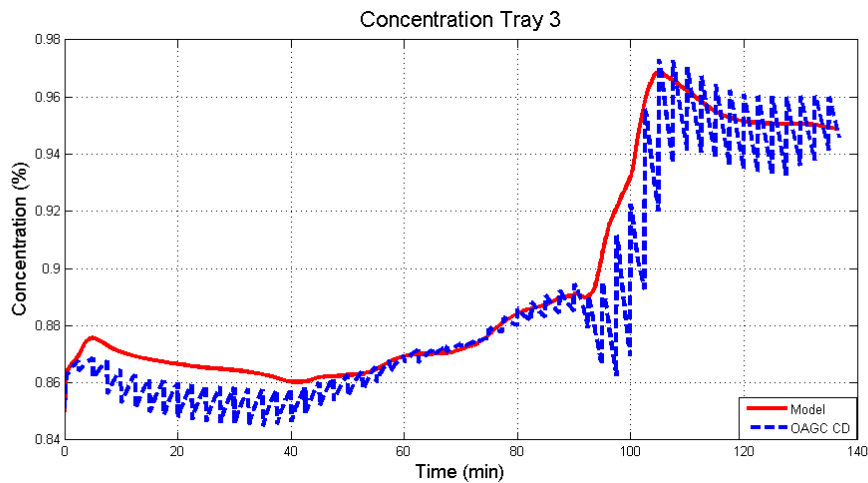FIGURE 5. Liquid composition in tray 3 ($T_s = T_e = 3s$)

FIGURE 6. Liquid composition in tray 12 ($T_s = T_e = 3s$)

FIGURE 7. Liquid composition in tray 3 ($T_s = T_e = 30s$)

FIGURE 8. Liquid composition in tray 3 ($T_e = 2.5m$)

5 percent in the worst case) considering the simplicity of the model used in the observer design. It can be seen in Figures 4 and 6 that the estimates $\hat{x}_1$ and $\hat{x}_{12}$ converge better than $\hat{x}_3$ towards the measured values. This is a normal occurrence, considering that x_1 and x_{12} are the measured process outputs (the observer inputs).

In a different experiment, but considering same initial, input and operating conditions, the sampling time was increased to $30s$. As can be seen in Figure 7, the continuous-discrete observer properly converges to the reference signal, whereas the discrete observer does not estimate the light composition properly (the estimated value is not even close to the measured one, so it does not appear in the figure). For the sake of simplicity only Tray 3 is depicted.

Different sampling times were used to validate de continuous discrete observer performance. Figures 8 and 9 show the estimated values for $T_e = 2.5$ and 5 minutes, respectively. As can be seen, the observer can estimate the light component of the mixture regardless the sampling time, however, the longer the sampling time the bigger the estimation error.

5. **Conclusions.** In this work, a continuous-discrete observer used to estimate the light component of a binary mixture in a distillation column was presented. One of the main
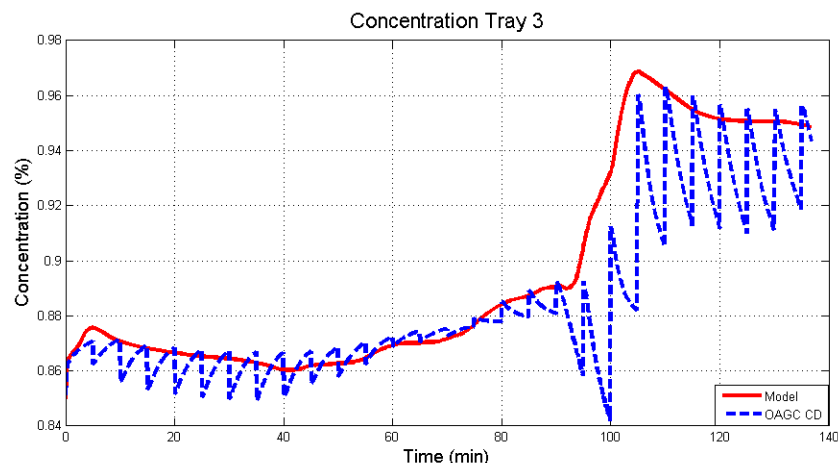
FIGURE 9. Liquid composition in tray 3 ($T_e = 5m$)

advantages of this observer is that it can be used for slow-dynamic processes, such as distillation, where the reference data can be measured using long sampling times without affecting the observer operation, unlike the discrete observer, where a long sampling time can cause an undesirable behavior.

Several experiments where performed in order to validate the continuous-discrete observer performance compared to the discrete one. The continuous-discrete version of the observer has an adequate performance regardless the sampling time, however, the estimation error increases if the sampling time is increased. It is necessary to experimentally determine the maximum sampling time in order to obtain an adequate estimation of the light composition of the mixture.

The obtained results demonstrate the adequate performance of the continuous-discrete observer under different sampling time conditions. In addition, the constant gain feature of the observer, allows to tune easily the parameters of the observer, making it suitable for its on-line application.

REFERENCES

[1] A. K. Jana, A. N. Samanta and S. Ganguly, Observer-based control algorithms for a distillation column, *Chem. Eng. Sci.*, vol.61, no.12, pp.4071-4085, 2006.

[2] W. Y. Wang, I.-H. Li, M. C. Chen, S. F. Su and Y. G. Leu, New time-efficient structure for observer-based adaptive fuzzy-neural controllers for nonaffine nonlinear systems, *International Journal of Innovative Computing, Information and Control*, vol.6, no.3(A), pp.963-978, 2010.

[3] F. Pierri, G. Paviglianiti, F. Caccavale and M. Mattei, Observer-based sensor fault detection and isolation for chemical batch reactors, *Eng. Appl. Artif. Intell.*, vol.21, no.8, pp.1204-1216, 2008.

[4] S. Manuja, S. Narasimhan and S. Patwardhan, Unknown input modeling and robust fault diagnosis using black box observers, *J. Process Control*, vol.19, no.1, pp.25-37, 2009.

[5] Z. Mao and B. Jiang, Fault identification and fault-tolerant control for a class of networked control systems, *International Journal of Innovative Computing, Information and Control*, vol.3, no.5, pp.1121-1130, 2007.

[6] S. Tong, T. Wang and W. Zhang, Fault tolerant control for uncertain fuzzy systems with actuator failures, *International Journal of Innovative Computing, Information and Control*, vol.4, no.10, pp.2461-2474, 2008.

[7] S. A. Velardi, H. Hammouri and A. A. Barresi, In-line monitoring of the primary drying phase of the freeze-drying process in vial by means of a Kalman filter based observer, *Chem. Eng. Res. Des.*, vol.87, no.10, pp.1409-1419, 2009.

[8] T. Ahmed-Ali, G. Kenné and F. Lamnabhi-Lagarrigue, Identification of nonlinear systems with time-varying parameters using a sliding-neural network observer, *Neurocomputing*, vol.72, no.7-9, pp.1611-1620, 2009.

[9] C. Delattre, D. Dochain and J. Winkin, Observability analysis of nonlinear tubular (bio)reactor models: A case study, *J. Process Control*, vol.14, no.6, pp.661-669, 2004.

[10] N. Sheibat-Othman, D. Peycelon, S. Othman, J. M. Suau and G. Févotte, Nonlinear observers for parameter estimation in a solution polymerization process using infrared spectroscopy, *Chem. Eng. J.*, vol.140, no.1-3, pp.529-538, 2008.

[11] C. M. Astorga-Zaragoza, V. M. Alvarado-Martínez, A. Zavala-Río, R. M. Méndez-Ocaña and G. V. Guerrero-Ramírez, Observer-based monitoring of heat exchangers, *ISA Trans.*, vol.47, no.1, pp.15-24, 2008.

[12] S. Ibrir, Circle-criterion approach to discrete-time nonlinear observer design, *Automatica*, vol.43, no.8, pp.1432-1441, 2007.

[13] E. E. Yaz, C. S. Jeong, A. Bahakeem and Y. I. Yaz, Discrete-time nonlinear observer design with general criteria, *J. Frankl. Inst. Eng. Appl. Math.*, vol.344, no.6, pp.918-928, 2007.

[14] V. Sundarapandian, Reduced order observer design for discrete-time nonlinear systems, *Appl. Math. Lett.*, vol.19, no.10, pp.1013-1018, 2006.

[15] M. Boutayeb and M. Darouach, A reduced-order observer for non-linear discrete-time systems, *Syst. Control Lett.*, vol.39, no.2, pp.141-151, 2000.

[16] F. Deza, E. Busvelle, J. P. Gauthier and D. Rakotopara, High gain estimation for nonlinear systems, *Syst. Control Lett.*, vol.18, no.4, pp.295-299, 1992.

[17] M. Nadri, H. Hammouri and C. Astorga, Observer design for continuous-discrete time state affine systems up to output injection, *European J. Control*, vol.10, no.3, pp.252-263, 2004.

[18] G. Goffaux, A. Vande-Wouwer and O. Bernard, Improving continuous-discrete interval observers with application to microalgae-based bioprocesses, *J. Process Control*, vol.19, no.7, pp.1182-1190, 2009.

[19] C. M. Astorga, N. Othman, S. Othman, H. Hammouri and T. F. McKenna, Nonlinear continuous-discrete observers: Application to emulsion polymerization reactors, *Control Eng. Pract.*, vol.10, no.1, pp.3-13, 2002.

[20] C. D. Immanuel and F. J. Doyle-III, Hierarchical multiobjective strategy for particle-size distribution control, *AICHE Journal*, vol.49, no.9, pp.2383-2399, 2003.

[21] T. Ahmed-Ali, R. Postoyan and F. Lamnabhi-Lagarrigue, Continuous-discrete adaptive observers for state affine systems, *Automatica*, vol.45, no.12, pp.2986-2990, 2009.

[22] H. Hammouri, B. Targui and F. Armanet, High gain observer based on a triangular structure, *Int. J. Robust Nonlinear Control*, vol.12, no.6, pp.497-518, 2002.

[23] S. Ben-Amor, *Observation et Commande de Systemes non Lineaires Temps-discret*, Ph.D. Thesis, Université Claude Bernard Lyon 1, Villeurbanne, France, 1997.

[24] D. G. Olsen, B. R. Young and W. Y. Svrcek, A study in advanced control application to an azeotropic distillation column within a vinyl acetate monomer process design, *Asia-Pac. J. Chem. Eng.*, vol.10, no.1-2, pp.47-60, 2002.

[25] E. Quintero-Mármol, W. L. Luyben and C. Georgakis, Application of an extended Luenberger observer to the control of multicomponent batch distillation, *Ind. Eng. Chem. Res.*, vol.30, no.8, pp.1870-1880, 1991.

[26] L. Fortuna, S. Graziani and M. G. Xibilia, Soft sensors for product quality monitoring in debutanizer distillation columns, *Control Eng. Pract.*, vol.13, no.4, pp.499-508, 2005.

[27] F. Viel, D. Bossanne, E. Busvelle, F. Deza and J. P. Gauthier, A new methodology to design extended Kalman filter application to distillation columns, *Proc. of the 31th IEEE Conf. on Decision & Control*, Tucson, Arizona, pp.2594-2595, 1992.

[28] F. Deza, E. Busvelle and J. P. Gauthier, Exponentially converging observers and internal stability using dynamic output feedback for distillation columns, *Chem. Eng. Science*, vol.47, no.15-16, pp.3935-3941, 1992.

[29] A. C. Téllez-Anguiano, F. Rivas-Cruz, C. M. Astorga-Zaragoza, E. Alcorta-García and D. Juárez-Romero, Process control interface system for a distillation plant, *Comput. Stand. Interfaces*, vol.31, no.2, pp.471-479, 2009.

[30] D. W. Green and R. H. Perry, *Perry's Chemical Engineers Handbook*, 8th Edition, McGraw-Hill, New York, 2008.

Appendix. Nomenclature.

Subscripts
f feeding tray
i tray number
n total number of trays
p tray number
R rectifying section
S stripping section

Lowercase letters
b_v bottom valve opening, $[0, 1]$
f feeding tray
i tray number
n total number of trays
p tray number
q_F quality of the feed
r_v reflux valve opening, $[0, 1]$
v volume ml^3
w weight fraction
x liquid compositions
x^{eq} liquid compositions in equilibrium
y vapor compositions
y^{eq} vapor compositions in equilibrium
z_f feed composition

Capital letters
B bottom product, mol/min
C_p specific heat, $kJ/mol°C$
D distilled product, mol/min
E Murphree's efficiency
F molar flow of the feeding stream, mol/min
F_V volumetric flow of the feeding stream, mL/min
K equilibrium constant
L liquid molar flow, mol/min
L_R liquid molar flow (rectifying section), mol/min
L_S liquid molar flow (stripping section), mol/min
M molar hold-up, mol
P^{sat} partial pressure (saturation), kPa
P_T total pressure, kPa
Q_b heating power, $Watts$
T temperature, $°C$
T_b boiling temperature, $°C$
T_F feeding temperature, $°C$
V vapor molar flow, mol/min
V_R vapor molar flow (rectifying section), mol/min
V_S vapor molar flow (stripping section), mol/min
W molecular weight, g

Greek letters
ρ component density, g/cm^3